AMERICAN SOCIETY FOR MICROBIOLOGY | Applied and Environmental Microbiology®

ENVIRONMENTAL MICROBIOLOGY

Alternative Sigma Factor RpoX Is a Part of the RpoE Regulon and Plays Distinct Roles in Stress Responses, Motility, Biofilm Formation, and Hemolytic Activities in the Marine Pathogen *Vibrio alginolyticus*

Dan Gu,[a,c] Jun Zhang,[a] Yuan Hao,[a] Rongjing Xu,[d] Yuanxing Zhang,[a,b] Yue Ma,[a,b] Qiyao Wang[a,b]

[a]State Key Laboratory of Bioreactor Engineering, East China University of Science and Technology, Shanghai, China

[b]Shanghai Engineering Research Center of Maricultured Animal Vaccines, Shanghai, China

[c]Jiangsu Key Laboratory of Zoonosis/Jiangsu Co-Innovation Center for Prevention and Control of Important Animal Infectious Diseases and Zoonoses, Yangzhou University, Yangzhou, China

[d]Yantai Tianyuan Aquatic Co. Ltd., Yantai, Shandong, China

ABSTRACT *Vibrio alginolyticus* is one of the most abundant microorganisms in marine environments and is also an opportunistic pathogen mediating high-mortality vibriosis in marine animals. Alternative sigma factors play essential roles in bacterial pathogens in the adaptation to environmental changes during infection and the adaptation to various niches, but little is known about them for *V. alginolyticus*. Our previous investigation indicated that the transcript level of the gene *rpoX* significantly decreased in an RpoE mutant. Here, we found that *rpoX* was highly expressed in response to high temperature and low osmotic stress and was under the direct control of the alternative sigma factor RpoE and its own product RpoX. Moreover, transcriptome sequencing (RNA-seq) results showed that RpoE and RpoX had different regulons, although they coregulated 105 genes at high temperature (42°C), including genes associated with biofilm formation, motility, virulence, regulatory factors, and the stress response. RNA-seq and chromatin immunoprecipitation sequencing (ChIP-seq) analyses as well as electrophoretic mobility shift assays (EMSAs) revealed the distinct binding motifs of RpoE and RpoX proteins. Furthermore, quantitative real-time reverse transcription-PCR (qRT-PCR) analysis also confirmed that RpoX can upregulate genes associated with flagella, biofilm formation, and hemolytic activities at higher temperatures. *rpoX* abrogation does not appear to attenuate virulence toward model fish at normal temperature. Collectively, data from this study demonstrated the regulatory cascades of RpoE and an alternative sigma factor, RpoX, in response to heat and osmotic stresses and their distinct and overlapping roles in pathogenesis and stress responses in the marine bacterium *V. alginolyticus*.

IMPORTANCE The alternative sigma factor RpoE is essential for the virulence of *Vibrio alginolyticus* toward marine fish, coral, and other animals in response to sea surface temperature increases. In this study, we characterized another alternative sigma factor, RpoX, which is induced at high temperatures and under low-osmotic-stress conditions. The expression of *rpoX* is under the tight control of RpoE and RpoX. Although RpoE and RpoX coregulate 105 genes, they are programming different regulatory functions in stress responses and virulence in *V. alginolyticus*. These findings illuminated the RpoE-RpoX-centered regulatory cascades and their distinct and overlapping regulatory roles in *V. alginolyticus*, which facilitates unraveling of the mechanisms by which the bacterium causes diseases in various sea animals in response to temperature fluctuations as well as the development of appropriate strategies to tackle infections by this bacterium.

Citation Gu D, Zhang J, Hao Y, Xu R, Zhang Y, Ma Y, Wang Q. 2019. Alternative sigma factor RpoX is a part of the RpoE regulon and plays distinct roles in stress responses, motility, biofilm formation, and hemolytic activities in the marine pathogen *Vibrio alginolyticus*. Appl Environ Microbiol 85:e00234-19. https://doi.org/10.1128/AEM.00234-19.

Editor Maia Kivisaar, University of Tartu

Address correspondence to Yue Ma, mymarine@ecust.edu.cn, or Qiyao Wang, oaiwqiyao@ecust.edu.cn.

D.G. and J.Z. contributed equally to this work.

Received 30 January 2019
Accepted 20 April 2019
Accepted manuscript posted online 3 May 2019
Published 1 July 2019

KEYWORDS ChIP-seq, RNA-seq, RpoE, RpoX, *Vibrio alginolyticus*, virulence

The Gram-negative bacterium *Vibrio alginolyticus* is a halophilic bacterium that is mainly found in marine and estuarine environments, causing high-mortality outbreaks of vibriosis in sea animals; this bacterium is also a notorious foodborne pathogen for humans (1, 2). Similar to other bacteria, the virulence of *V. alginolyticus* is strictly regulated by environmental factors such as cell density and temperature (3). In our previous study, we reported that the genes involved in the main virulence-associated characteristics of *V. alginolyticus*, such as biofilm formation, motility, extracellular proteases (Asp, Pep, and MviN), siderophore-dependent iron uptake systems, and type III and VI secretion systems (T3SS and T6SS), are tightly regulated by quorum sensing (QS) (4–10).

Alternative sigma (σ) factors are global regulators that enable the expression of genes associated with stress adaptation and virulence in response to diverse stimuli in both the environment and the host in vibrios (11–13). Our previous investigation demonstrated that the temperature-dependent binding of RpoE to distinct promoters appears to underlie a σ^E-controlled switch between the expression of virulence genes and adaptation to thermal stress (3). The RpoE protein is essential for the growth of *V. alginolyticus*, *V. cholerae*, and *V. parahaemolyticus* at high temperatures (3, 14–16). RpoS is another well-characterized alternative sigma factor, which controls virulence and cellular responses to reactive oxygen species (ROS), starvation, DNA damage, extreme temperatures, ethanol, and hyperosmolarity (17–19). In *V. alginolyticus*, RpoS is part of the regulatory networks of virulence and the LuxS quorum-sensing system and responds to high-temperature stress (20). In addition, the alternative sigma factor RpoH activates the transcription of genes involved in the heat shock response in various bacterial species, including vibrios (21). The RpoE protein can directly bind to the promoter of *rpoH* and activate its expression to respond and adapt to high-temperature conditions in vibrios (3, 22). In *V. alginolyticus*, the gene *rpoX*, annotated to encode an RpoS-like alternative sigma factor, was recently implicated as being involved in stress adaptation (23). The detailed regulatory roles associated with *rpoX* as well as the underlying mechanisms remain unclear.

Our recent transcriptomic analysis of *V. alginolyticus* identified that *rpoX* was significantly downregulated in the *rpoE* mutant (3). In this study, we characterized the roles of the *rpoX* gene in adaptation to heat stress and the regulation of virulence gene expression. The expression of *rpoX* was under the strict control of RpoE in response to high temperature and low osmotic stress. In addition, the regulons of RpoE and RpoX were defined with transcriptome sequencing (RNA-seq) and chromatin immunoprecipitation sequencing (ChIP-seq) analyses to illuminate their distinct and overlapping regulatory roles in the stress response, biofilm formation, motility, hemolytic activity, and virulence. These data enriched our understanding of the basis and regulatory networks of vibrio adaptation to osmosis, heat, and other stresses.

RESULTS

RpoX is induced by high temperature and low osmotic stress. A BLASTP analysis showed that the RpoX protein contains three conserved functional domains: sigma 70 region 1.2 (residues 27 to 59), sigma 70 region 2 (residues 65 to 125), and sigma 70 region 4 (residues 230 to 287) (see Fig. S1A in the supplemental material). In addition, an analysis of the conserved functional domains of the RpoE, RpoH, RpoS, and RpoD proteins from *V. alginolyticus* indicated that even though the RpoX protein was initially annotated as an RpoS-like sigma factor (23), this protein lacked the featured sigma region 3 of the RpoS protein. In addition, the three conserved domains of RpoX were highly similar (with 27% identity and 45% similarity) to the RpoH sigma factor, which could be directly modulated by the RpoE protein and was responsive to high-temperature stress (Fig. S1A). The BLASTP analysis also indicated that the *V. alginolyticus* RpoX protein shared 99%, 83%, and 78% identities with the homologous proteins

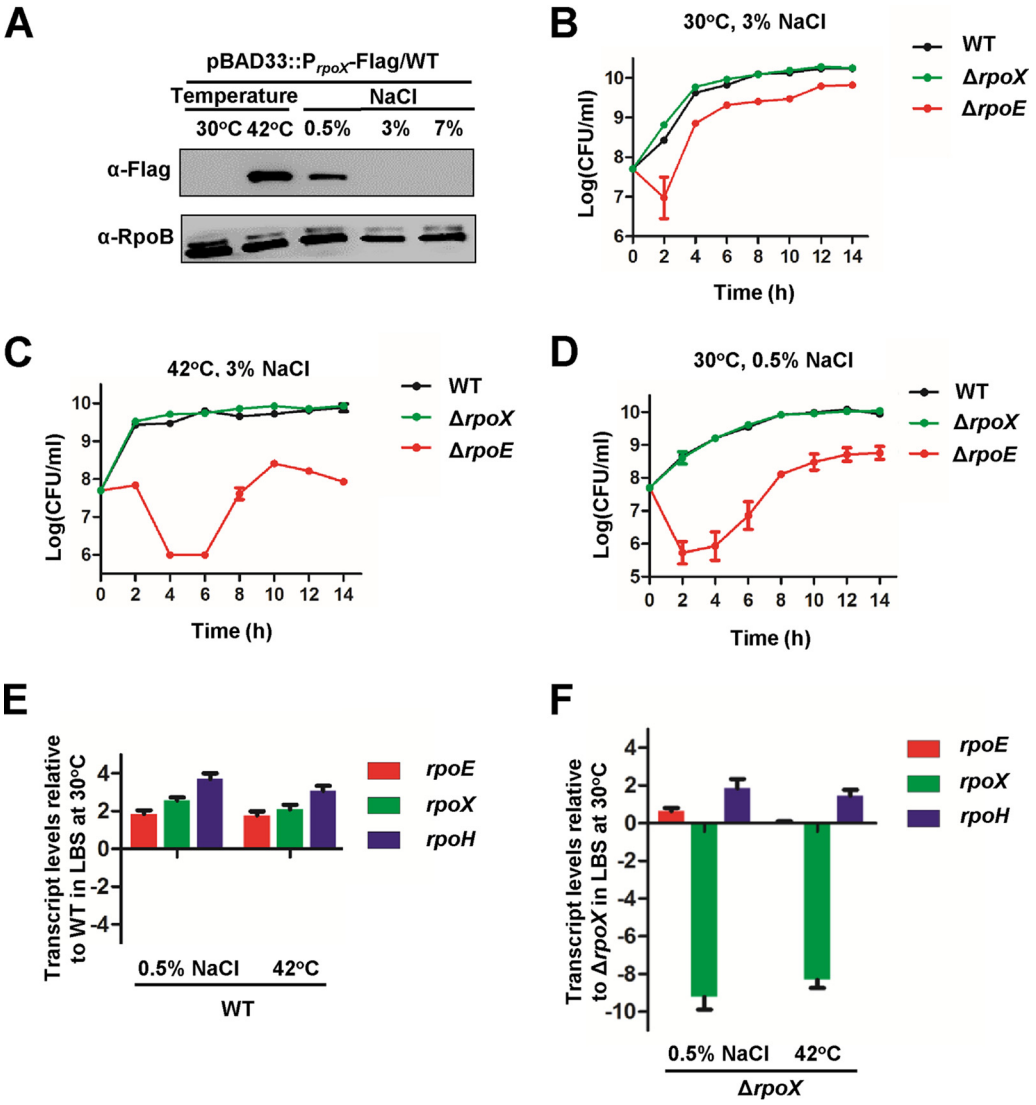

FIG 1 Stress-responsive *rpoX* expression in *V. alginolyticus*. (A) Western blot assay of RpoX levels in *V. alginolyticus* strains grown under various temperature or osmotic conditions. A Flag-tag-specific antibody was used to probe WT cells expressing RpoX-Flag driven by the native *rpoX* promoter. RpoB was used as a loading control. (B to D) Growth curves of WT, Δ*rpoX*, and Δ*rpoE* strains in LB medium containing 3% NaCl at 30°C, the normal growth conditions for this halophile (B); 3% NaCl at 42°C (C); and 0.5% NaCl at 30°C (D). Samples were taken and plate counted after serial dilutions with fresh LBS medium. (E and F) qRT-PCR analysis of the transcript levels of *rpoX*, *rpoE*, and *rpoH* in WT (E) and Δ*rpoX* (F) cells cultured under different stress conditions relative to WT and Δ*rpoX* cells grown in LBS medium at 30°C, respectively. Total RNA was isolated from the strains after 9 h of growth. The results are presented as the means ± standard deviations (SD) ($n = 3$).

Vp1393 from *V. parahaemolyticus*, A1Q_0985 from *V. harveyi*, and ATB83_RS10190 from *V. splendidus*, respectively (Fig. S1B). These analyses indicated that RpoX is highly conserved in these bacteria and might be an important part of the RpoE regulon.

Our previous study indicated that the RpoE protein contributed to different stress responses in *V. alginolyticus*, such as the responses to high-temperature stress, osmotic stress, and H_2O_2 (3), and the *rpoS* mutant strain of *V. alginolyticus* was also defective in resistance to environmental stresses (20). Although RpoX has been suggested to be involved in stress adaptations, its exact biological roles remain undetermined (23). Therefore, we first examined the expression of RpoX under various stress conditions with a *V. alginolyticus* strain carrying an *rpoX* promoter reporter. RpoX protein could be expressed at a high temperature (42°C) and under low-osmotic-stress conditions (0.5% NaCl) (Fig. 1A). The growth of the wild-type (WT), Δ*rpoE*, and Δ*rpoX* strains was monitored at 30°C (Fig. 1B) and 42°C (Fig. 1C) in Luria-Bertani (LB) broth containing 3%

NaCl and at 30°C in LB broth containing 0.5% NaCl (Fig. 1D), respectively. The severely impaired growth of *V. alginolyticus* at 42°C in LB broth containing 0.5% NaCl excluded further experiments under these conditions. The Δ*rpoE* strain had a marked growth reduction under its optimal growth conditions (30°C with 3% NaCl) (Fig. 1B) and had a longer lag phase and reached a drastically lower stationary-phase growth rate than the WT strain at 42°C and in 0.5% NaCl (Fig. 1B to D). However, the Δ*rpoX* strain did not exhibit a significant difference in growth compared to the WT strain under these conditions (Fig. 1B to D). These investigations indicated that the RpoX protein can be induced at 42°C and in 0.5% NaCl but might not be required for the survival of *V. alginolyticus* under these conditions.

The RpoE sigma factor can directly regulate the expression of RpoH (3), which shares the same functional domains as the RpoX protein and responds to different types of stress. Therefore, we suspect that the Δ*rpoX* strain did not exhibit decreased survival at 42°C and in 0.5% NaCl due to induction of the expression of *rpoH* in the Δ*rpoX* strain, which might rescue bacterial growth under these stress conditions. After the failure of the trials to generate an *rpoH* deletion or null mutant to test this hypothesis, we resorted to detection of the expression of *rpoE*, *rpoX*, and *rpoH* in the WT and Δ*rpoX* strains at 42°C and in 0.5% NaCl. Indeed, the expression of *rpoE*, *rpoX*, and *rpoH* markedly increased in the WT strain cultured in 0.5% NaCl and at 42°C (Fig. 1E). In the *rpoX* mutant strain, the transcription level of *rpoH* in 0.5% NaCl and at 42°C was ~2-fold higher than that under culture conditions of 3% NaCl at 30°C, while the transcription of *rpoE* exhibited no significant difference between both culture conditions (Fig. 1F), which indicated that the increased expression of *rpoH* might compensate for the abrogation of RpoX protein to regulate the responses to these stress factors in the Δ*rpoX* strain. Moreover, these data also suggested that *rpoX* might be involved in the transcription of *rpoE*. Taken together, these findings suggested that RpoX is induced by and might be involved in the stress response to 42°C (high temperature) and 0.5% NaCl (low-osmotic-stress conditions).

RpoE and RpoX directly bind to the *rpoX* promoter and activate its transcription. Based on sequence analysis, the *rpoX* promoter region contains the conserved −35 motif "GCACTTT," the −10 motif "TGCTCA" for an RpoE-binding site (Fig. 2A), and the predicted transcriptional start site +1A. However, a 5′ rapid amplification of cDNA ends (RACE) study found another transcriptional start site, +1G (Fig. 2A), which is located 104 bp downstream of the predicted RpoE-binding site, so we suggested that another promoter sequence might exist in the *rpoX* promoter. In addition, sequence analysis showed another putative sigma factor-binding sequence (TGTCTACA/ATA TAAA [−35/−10 motifs]), which was located directly upstream of the transcriptional start site +1G, and we speculate that this site might be the specific binding site of the RpoX protein (Fig. 2A). Overall, the sequence analysis showed that the *rpoX* promoter contains two conserved binding sites. An electrophoretic mobility shift assay (EMSA) was then used to determine whether the RpoE and RpoX proteins could directly bind to the *rpoX* promoter. As expected, the RpoE protein bound directly to the *rpoX* promoter region in a concentration-dependent manner in the presence of high concentrations (10-fold) of a nonspecific poly(dI-dC) competitor, and the RpoE protein could not bind to a negative-control DNA (Fig. 2B). In addition, the EMSA results also showed that the RpoX protein bound directly to its own promoter (Fig. 2C).

Given the direct interaction of the RpoE and RpoX proteins with the promoter of *rpoX*, we next determined whether the RpoE and RpoX proteins could regulate the expression of *rpoX in vivo*. We transformed the pBAD33::P_{rpoX}-Flag plasmid into WT, Δ*rpoE*, and Δ*rpoX* strains, and Western blotting confirmed that the expression of RpoX markedly decreased in the Δ*rpoX* mutant but was abolished in the Δ*rpoE* strain at 42°C (Fig. 2D). Taken together, these results show that the expression of *rpoX* was directly regulated by the sigma factors RpoE and RpoX.

Global analyses of the regulons of RpoE and RpoX in *V. alginolyticus*. Because RpoE and RpoX were found to be important in the response to high temperatures, we

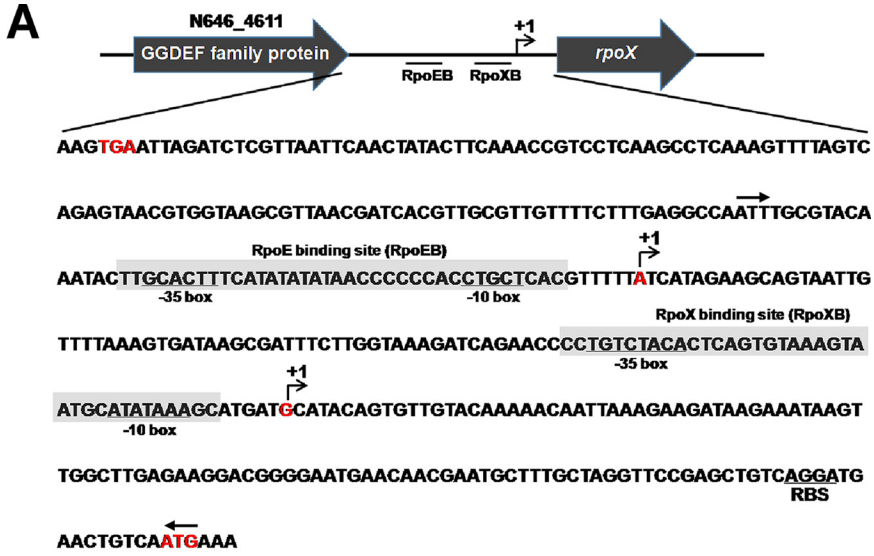

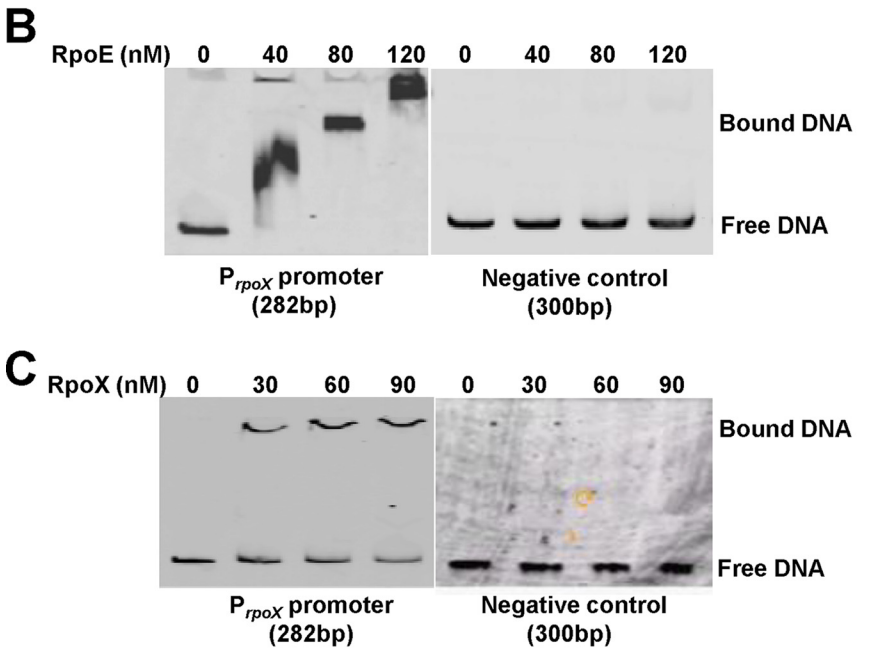

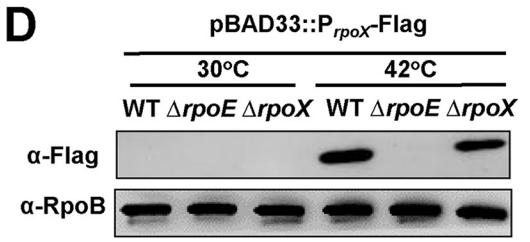

FIG 2 RpoE and RpoX directly bind to the *rpoX* promoter. (A) Diagram showing the promoter region of the *rpoX* gene. The RpoE- and RpoX-binding sites and the ribosome-binding site (RBS) are underlined. The regions protected by RpoE/RpoX are shadow boxed. The transcription start sites are labeled as +1 and marked in red. The red letters "TGA" and "ATG" are the stop codon of N646_4611 and the start codon of *rpoX*, respectively. (B and C) EMSA of RpoE and RpoX specifically binding to the *rpoX* promoter. Various concentrations of the RpoE and RpoX proteins were added to mixtures of poly(dI-dC) and Cy5-labeled *rpoX* promoter DNA (a 282-bp fragment of the promoter adjoining the start codon "ATG," as indicated with the pair of arrows above the sequence). The same reactions were also carried out for a 300-bp fragment of the *gyrB* promoter region (negative control), which cannot be bound by RpoX and RpoE. (D) Western blotting of RpoX levels in WT, Δ*rpoE*, and Δ*rpoX* cells harboring pBAD33::P_{rpoX}-Flag and grown at normal (30°C) or high (42°C) temperatures. RpoB was used as a loading control for the blots.

identified genes that are regulated by RpoE and RpoX at high temperatures by comparing the transcriptomes of the WT, Δ*rpoX*, and Δ*rpoE* strains at 42°C. The results showed that many genes were regulated by the RpoE and RpoX proteins at high temperatures (the 50 most upregulated and most downregulated genes are listed in Table 1). Comparison of the RNA-seq data for the WT and Δ*rpoE* strains at 42°C showed that 393 (8.4%) and 440 (9.4%) of the annotated genes were up- and downregulated ($\log_2$ fold change [$\log_2$FC] ≥ 2 or $\log_2$FC ≤ -2; $P < 0.001$), respectively, in the Δ*rpoE* strain (Fig. 3A). In addition, comparison of the RNA-seq data for the WT and Δ*rpoX* strains at 42°C showed that 240 (5.1%) and 408 (8.7%) genes were up- and downregulated ($\log_2$FC ≥ 2 or $\log_2$FC ≤ -2; $P < 0.001$), respectively, in the Δ*rpoX* strain (Fig. 3B). To identify the coregulon of RpoE and RpoX, we compared the RNA-seq data and identified 105 overlapping genes between the regulons of RpoE and RpoX (Fig. 3C), including genes associated with biofilm formation, motility, and stress adaptation. These data suggested that both the RpoE and RpoX proteins are global regulators in *V. alginolyticus* in response to high-temperature stress.

The data presented in Fig. 3D and E describe the expression patterns of genes that are potentially associated with virulence (including genes associated with biofilm formation, motility, and virulence), regulatory factors, and stress responses. Our previous study showed that the RpoE protein can regulate motility and virulence (3), and the RNA-seq data confirmed that *rpoX* transcription could be positively regulated (fold change of −2.4) by RpoE. In addition, the RpoX protein controls the expression of various genes involved in biofilm formation and motility, virulence-associated genes, and regulatory factors. Finally, we also found that the RpoX protein is involved in the stress response ($n = 15$) via the regulation of heat shock and cold shock proteins, outer membrane proteins, and proteins associated with multidrug resistance. Taken together, our results demonstrated that RpoE and RpoX are important regulatory factors at high temperatures and are responsible for the regulation of virulence-associated genes.

RpoE- and RpoX-binding motifs. The binding motifs of RpoE and RpoX were generated by the MEME-suite tool (http://meme-suite.org) in search of the regulated genes' promoter regions in the identified regulon of RpoE and RpoX. As shown in Fig. 4A, the −10 box and −35 box were identified, and the conserved binding site of RpoE was found to be similar to the established RpoE-binding site identified by ChIP-seq in other bacteria (24); the results of our previous study also showed a similar binding site for RpoE in the promoter of *luxR* (TGACCTT for the −35 region and TCATCA for the −10 region) (3). In addition, based on the RNA-seq data for RpoX at high temperatures, the conserved −35 box and −10 box of the RpoX-binding motif were also revealed (Fig. 4B), and the −35 box and −10 box sequences were similar to the predicted binding sites in the promoter of *rpoX* (TGTCTACA/ATATAAA) (Fig. 2A). The binding motifs show marked differences between the binding sites of the RpoE and RpoX sigma factors.

Identification of RpoX-binding regions by ChIP-seq. We further used ChIP-seq experiments to investigate the possible RpoX-binding loci on the chromosome of *V. alginolyticus* cultured at a high temperature (42°C) and under low-osmotic-stress conditions (0.5% NaCl). We identified 9 enriched loci (fold change of >2.0; $P < 0.01$) harboring RpoX-binding peaks at a high temperature (42°C) but only 2 enriched loci exhibiting peaks under low-osmotic-stress conditions (0.5% NaCl), and these 2 peaks were also included in the high-temperature peaks (Table 1). Only 4 of these 9 peaks were located in intergenic regions. We thus chose the 4 related regions for EMSAs. Among these enriched loci, the *rpoX* promoter was first identified as a binding substrate of RpoX with a fold enrichment of 10.9, and EMSAs also confirmed that the RpoX protein could directly bind to its own promoter (Fig. 2C). In addition, the additional 3 peaks upstream of N646_4603 (7.6-fold), N646_4601 (6.1-fold), and N646_1623 (4.8-fold) were found to be located in distinct promoter regions (Fig. 5A to C). As expected, EMSAs validated that the RpoX protein bound directly to these promoters in the presence of high concentrations (10-fold) of a nonspecific poly(dI-dC) competitor (Fig. 2C and Fig. 5A to C). The *gyrB* promoter region was used as the

TABLE 1 Genes coregulated by RpoE and RpoX at 42°C

Gene identification[a]	Annotation[b]	Fold change (Δ*rpoE*/WT)	Fold change (Δ*rpoX*/WT)	Promoter region bound by RpoX determined by ChIP-seq[c]	Virulence-associated gene[d]
N646_4603	Hypothetical protein	−175.96	−1,081.83	Y	
N646_4599	Hypothetical protein	−14.42	−263.51		
N646_4604	Hemolysin D	−21.50	−119.59	Y	Y
N646_0533	Anti-anti-sigma regulatory factor	−134.98	−108.89		Y
N646_3842	Hypothetical protein	−2.42	−104.79		
N646_4684	Hypothetical protein	−4.74	−79.41		
N646_4605	Hypothetical protein	−9.17	−55.37		
N646_3940	Hypothetical protein	−5.11	−47.04		
N646_0523	Putative membrane protein of ExoQ family, involved in exopolysaccharide production	−2.49	−42.23		Y
N646_4610	Hypothetical protein, RpoX	−4.44	−39.73	Y	Y
N646_1050	Hypothetical protein	−3.20	−31.18		
N646_4601	Hypothetical protein	−44.33	−29.20	Y	
N646_3768	Hypothetical protein	−6.06	−21.91		
N646_0526	Putative galactosyltransferase	−5.28	−19.04		
N646_4606	ABC transporter outer membrane component	−2.55	−17.99		
N646_1186	Sodium-type flagellar protein MotY	−2.35	−16.89		Y
N646_4602	Hypothetical protein	−29.71	−16.78		
N646_0512	FMN-dependent NADH-azoreductase	−2.68	−16.44		
N646_4598	Hypothetical protein	−6.38	−14.22		
N646_4600	Hypothetical protein	−31.74	−11.95	Y	
N646_0722	Hypothetical protein	−2.15	−11.33		
N646_2916	Hypothetical protein	−20.26	−10.69		
N646_2929	Polar flagellar FlgF	−2.52	−10.37		Y
N646_1399	Hypothetical protein	−1.41	−10.16		
N646_4608	Hypothetical protein	−3.93	−10.07		
N646_1161	Hypothetical protein	−3.12	−9.17		
N646_1591	Hypothetical protein	−2.23	−8.63		
N646_0708	Putative acetyltransferase	−5.03	−8.55		
N646_4609	Hypothetical protein	−4.83	−8.51	Y	
N646_3939	Hypothetical protein	−3.08	−7.66		
N646_0532	Hypothetical protein	−32.48	−7.18		
N646_0389	Hypothetical protein	−4.52	−6.73		
N646_0390	Hypothetical protein	−4.98	−6.44		
N646_0562	Hypothetical protein	−4.71	−6.43		
N646_0384	Putative dioxygenase	−2.40	−6.38		
N646_3470	GTP cyclohydrolase II	−2.57	−6.38		
N646_0714	Transcriptional regulator, GntR family protein	−2.75	−6.24		
N646_4629	Cytochrome *c* oxidase, subunit II	−2.03	−5.99		
N646_1446	50S ribosomal protein L31	−0.46	−5.88		
N646_0176	Hypothetical protein	−2.28	−5.39		
N646_0385	2-Keto-4-pentenoate hydratase/2-oxohepta-3-ene-1,7-dioic acid hydratase	−2.42	−4.98		
N646_3844	Pirin-related protein	−2.69	−4.98		
N646_0013	Hypothetical protein	−111.19	−4.81		
N646_4302	Hypothetical protein	−3.03	−4.81		
N646_0530	Putative capsular polysaccharide biosynthesis	−4.10	−4.59		Y
N646_2548	Glycerol dehydrogenase	−4.40	−4.31		
N646_1338	Flagellar biosynthesis protein FlhF	−5.32	−3.76		Y
N646_1844	Putative fimbrial assembly protein PilM	−2.05	−3.74		Y
N646_0713	Carboxyphosphonoenolpyruvate phosphonomutase	−2.70	−3.71		
N646_0456	Hypothetical protein	−2.36	−3.61		
N646_4031	Hypothetical protein	−7.04	−3.52		
N646_4030	Putative phenylacetate-CoA ligase	−8.34	−3.41		
N646_2724	DNA-binding response regulator PhoB	−2.33	−3.26		Y
N646_4032	Oxidoreductase	−6.58	−3.26		
N646_2270	Hypothetical protein	−3.55	−3.16		
N646_3227	CsuA	−22.07	−3.06		Y
N646_4508	Enoyl-CoA hydratase	−2.04	−2.99		
N646_0645	Amino acid ABC transporter, periplasmic amino-acid-binding protein	−2.64	−2.89		
N646_4675	Hypothetical protein	−2.06	−2.71		
N646_2932	Flagellar P-ring protein FlgI	−3.54	−2.67		Y
N646_0301	Hypothetical protein	−5.28	−2.67		

(Continued on next page)

TABLE 1 (Continued)

Gene identification[a]	Annotation[b]	Fold change (Δ*rpoE*/WT)	Fold change (Δ*rpoX*/WT)	Promoter region bound by RpoX determined by ChIP-seq[c]	Virulence-associated gene[d]
N646_4059	Hypothetical protein	−2.10	−2.66		
N646_2799	Small protein A	−2.16	−2.60		
N646_2936	Flagellin	−2.28	−2.57		Y
N646_3225	CsuC	−15.77	−2.49		Y
N646_4417	Hypothetical protein	−10.82	−2.40		
N646_3072	Hypothetical protein	−2.52	−2.36		
N646_4028	Hypothetical protein	−14.67	−2.36		
N646_0455	Hypothetical protein	−2.10	−2.27		
N646_0799	Hypothetical protein	−3.72	−2.27		
N646_0531	Periplasmic protein involved in polysaccharide export	−16.16	−2.27		Y
N646_0807	Hypothetical protein	−2.45	−2.24		
N646_3224	CsuD	−5.06	−2.22		Y
N646_4029	Putative high-affinity branched-chain-amino-acid transport ATP-binding protein	−11.73	−2.21		
N646_0145	Tryptophanyl-tRNA synthetase	−2.99	−2.19		
N646_3223	CsuE	−2.97	−2.17		Y
N646_0685	Hypothetical protein	−3.58	−2.04		
N646_4419	Hypothetical protein	−2.18	−2.03		
N646_0561	Formate dehydrogenase accessory protein	−3.67	−2.00		
N646_0626	Hypothetical protein	5.81	2.05		
N646_2558	Hypothetical protein	2.20	2.05		
N646_0313	Imidazolonepropionase	2.47	2.07		
N646_2232	Hypothetical protein	3.12	2.10		
N646_3280	Pyruvate formate-lyase	2.88	2.10		
N646_1747	Aspartate carbamoyltransferase regulatory subunit	2.64	2.15		
N646_3214	Hypothetical protein	3.47	2.15		
N646_0304	Outer membrane protein	2.02	2.19		
N646_0641	Hypothetical protein	3.82	2.28		
N646_3434	Putative ribosomal protein *N*-acetyltransferase	2.58	2.39		
N646_2428	UTP-glucose-1-phosphate uridylyltransferase	2.36	2.47		
N646_4424	Hypothetical protein	2.15	2.47		
N646_4184	Hypothetical protein	2.06	2.56		
N646_3925	Putative acriflavine resistance protein	2.99	2.62		
N646_3664	Thermolabile hemolysin	2.75	2.65		Y
N646_4456	Putative KHG/KDPG aldolase	2.44	2.81		
N646_3202	Putative ABC transporter membrane-spanning permease	2.03	2.96		
N646_3782	Hypothetical protein	3.47	4.15		
N646_3806	Alcohol dehydrogenase, zinc-binding domain protein	3.66	4.21		
N646_3556	Putative hydrolase	3.26	5.04		
N646_2057	Hypothetical protein	2.95	5.26		
N646_4487	Arginine ABC transporter, periplasmic arginine-binding protein	11.25	5.30		
N646_3755	Putative muconate cycloisomerase I	2.24	6.51		
N646_3685	Hypothetical protein	5.67	7.51		
N646_3856	Hypothetical protein	3.03	7.62		
N646_3885	Glyceraldehyde-3-phosphate dehydrogenase	2.77	7.82		
N646_4611	Hypothetical protein	1.02	−1.27	Y	
N646_1623	50S ribosomal protein L19	1.09	2.37	Y	
N646_1624	tRNA (guanine-N^1)-methyltransferase	1.03	2.67	Y	

[a]All the genes with differential expression with a *P* value of <0.001.
[b]FMN, flavin mononucleotide.
[c]Y indicates that the promoter region of the gene was also bound by RpoX, as identified by ChIP-seq analysis.
[d]Y indicates that the gene was annotated as a virulence-associated genes.

negative control, and no peak was found in the promoter region of *gyrB* during ChIP analysis (Fig. 5D). Overall, four genes containing *rpoX*-binding sites were identified by EMSAs and ChIP-seq analysis. Among these four ChIP-identified promoter regions, *rpoX*, N646_4604 (N646_4603 and N646_4604 are in the same operon), and N646_4601 were positively regulated and N646_1623 was negatively regulated by RpoX, as revealed by

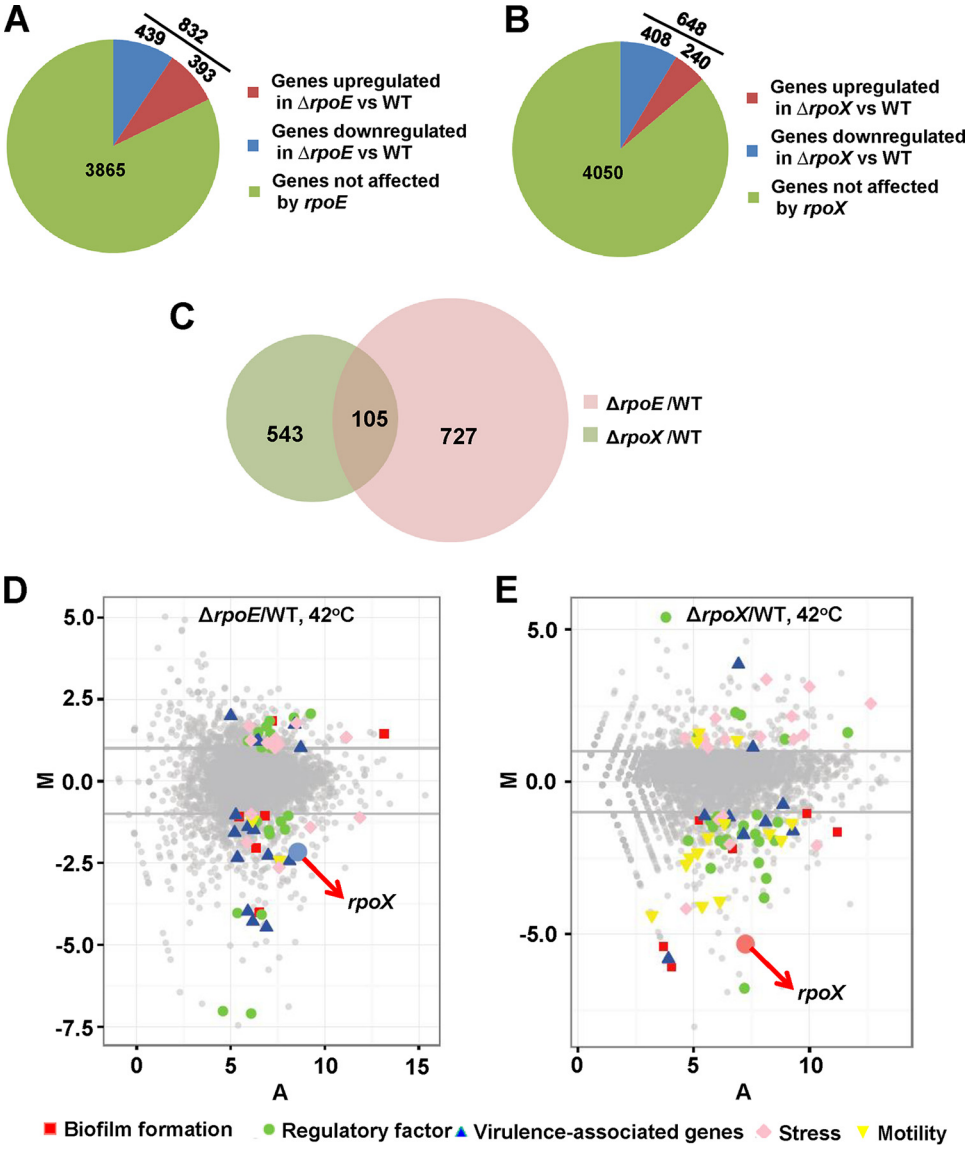

FIG 3 Comparative analyses of the transcriptional responses of *V. alginolyticus* to *rpoE* and *rpoX* abrogation at 42°C. (A and B) Pie charts representing genes differentially transcribed in Δ*rpoE* (A) and Δ*rpoX* (B) cells compared to WT cells grown in LBS medium at 42°C. (C) Venn diagrams showing overlapping genes with significantly increased or decreased transcript abundances (FC ≥ 2 or FC ≤ -2; adjusted *P* value [P_{adj}] of $<1 \times 10^{-2}$) in response to different culture conditions. (D and E) MA plots depicting changes in gene expression between Δ*rpoE* and WT strains (D) and between Δ*rpoX* and WT strains (E) in LBS medium at 42°C. The $\log_2$ value of the ratios of the abundances of each transcript between the two conditions (M) (*y* axis) is plotted against the average $\log_2$ value of the abundance of that transcript under both conditions (A) (*x* axis).

RNA-seq analysis. Interestingly, the gene N646_4604 encodes RTX-type hemolysin D (HlyD), and HlyD has been reported to be a hemolysin in other bacteria (25), further suggesting a role for RpoX in the pathogenesis of *V. alginolyticus*.

RpoX modulates biofilm formation, motility, and hemolytic activities in *V. alginolyticus*. In our RNA-seq analysis, we found that several flagellum-related genes were regulated by the RpoE and RpoX proteins. We thus further investigated the roles of *rpoX* in the motility of this bacterium. The swimming ability was significantly reduced in the Δ*rpoX* strain compared with the WT strain, and *rpoX* complementation restored the swimming ability at high temperatures (Fig. 6A); however, there was no significant difference in swarming abilities between the WT and Δ*rpoX* strains (Fig. 6A).

Furthermore, biofilm formation was significantly decreased in the Δ*rpoX* strain compared with the WT strain, and biofilm formation was restored when the *rpoX* gene was

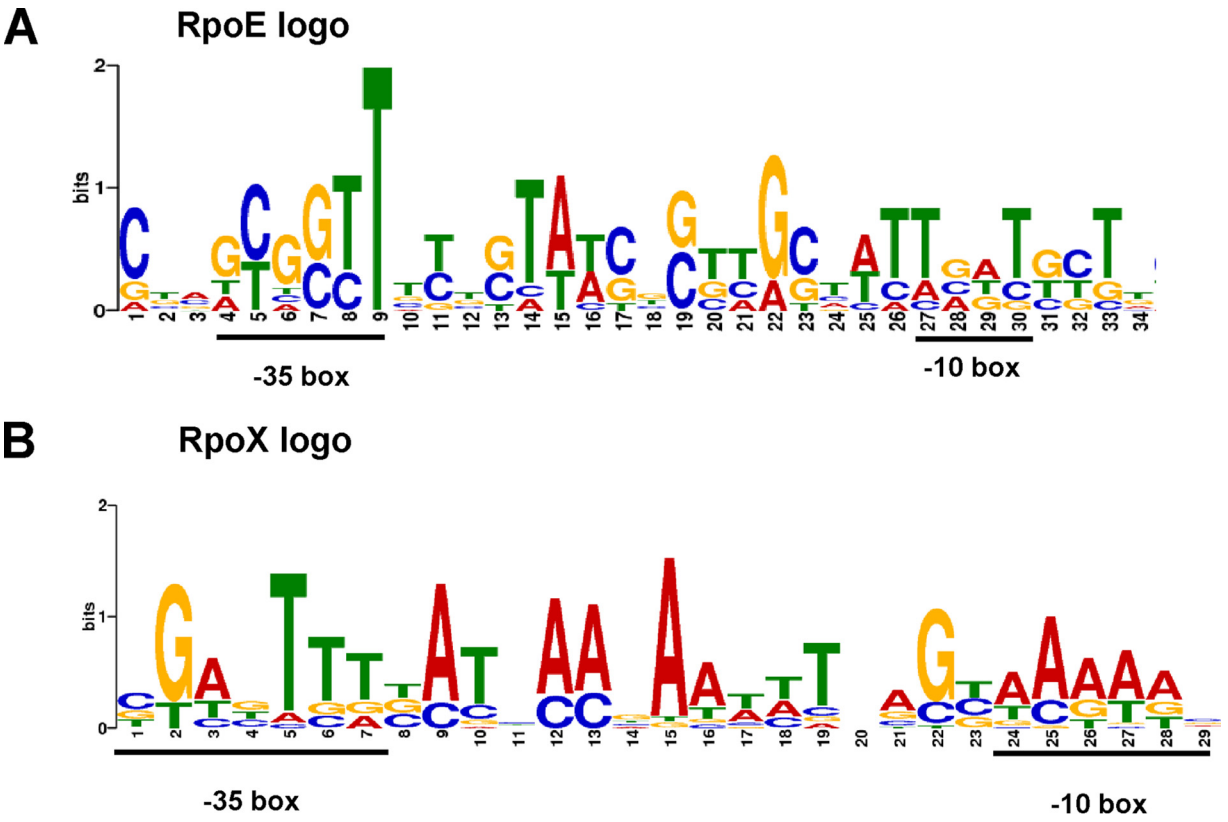

FIG 4 Conserved binding site of RpoE and RpoX generated by RNA-seq data. The most significant RpoE-binding motif (A) or RpoX-binding motif (B) was derived from an RNA-seq binding sequence generated by the MEME-suite tool. The height of each letter represents the relative frequency of each base at different positions in the consensus sequence.

complemented (Fig. 6B). As shown in Fig. 2A, N646_4611 encodes a GGDEF family protein and is located upstream of the *rpoX* gene; GGDEF family proteins have been identified as regulators of biofilm formation and motility (24). Therefore, we constructed a ΔN646_4611 mutant strain and an N646_4611-overexpressing strain driven by the pBAD promoter in the ΔN646_4611 mutant strain (N646_4611^{OE}/ΔN646_4611) with the induction of L-arabinose, which showed no apparent influence on *V. alginolyticus* biofilm formation. Biofilm formation was significantly reduced in the ΔN646_4611 mutant strain and enhanced in the N646_4611^{OE}/ΔN646_4611 strain (Fig. 6B). To determine whether RpoX regulates biofilm formation via N646_4611, we overexpressed the N646_4611 protein in the Δ*rpoX* strain, N646_4611^{OE}/Δ*rpoX*, and the level of biofilm formation by the strain was significantly lower than that by the N646_4611^{OE}/ΔN646_4611 strain but higher than that by the N646_4611^{OE}/Δ*rpoX* strain (Fig. 6B), which suggested that RpoX might not regulate biofilm formation via the N646_4611 protein. RNA-seq data showed that N646_4604, encoding RTX-type hemolysin D, was downregulated in the Δ*rpoX* strain. Δ*rpoX* cells showed weaker hemolytic activity than WT cells, and complementation of *rpoX* restored the activity to the WT level at 30°C and 42°C. The Δ*rpoE* mutant strain showed drastically reduced hemolytic activity similar to that of the Δ*hlyD* strain (Fig. 6C).

Quantitative real-time reverse transcription-PCR (qRT-PCR) was then further used to verify the roles of *rpoX* in the above-mentioned genes' expression. The results showed that flagellum-related genes (*flgD*, *flgC*, and *flgB*) were downregulated in the Δ*rpoX* strain compared with the WT strain, and the expression of these genes was restored to WT levels in the *rpoX*-complemented strain (Fig. 6D). Moreover, the expression of the exopolysaccharide biosynthesis- and biofilm formation-associated gene *exoQ* and the hemolysin-related gene *hlyD* was significantly downregulated in the Δ*rpoX* strain compared to the WT strain, and complementation restored the expression of these

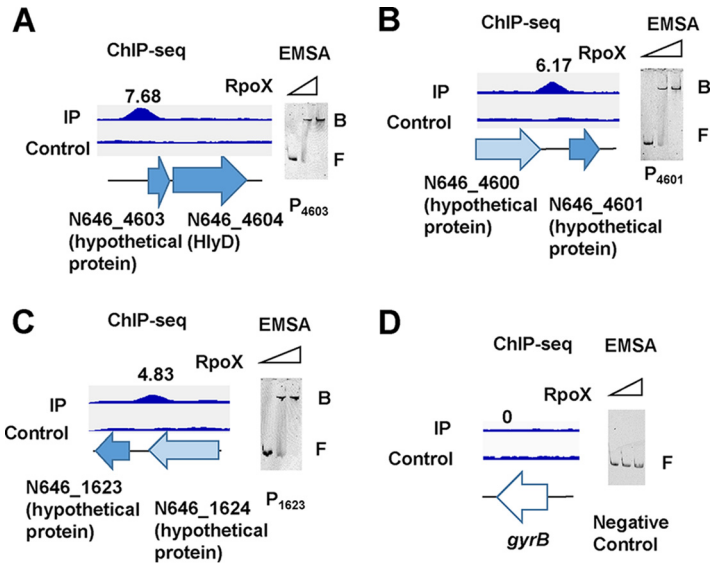

FIG 5 ChIP-seq analysis of genes directly bound and regulated by RpoX. (A to C) N646_4603 (A), N646_4601 (B), and N646_1623 (C) were used for peak comparison of ChIP-seq (left) and EMSA (right) results. The fold enrichment of each of the typical promoters bound by RpoX is shown. (D) A 300-bp fragment of the *gyrB* promoter region is shown as the negative control, which cannot be bound by RpoX. B, bound DNA; F, free DNA. The numbers above each of the peaks indicate the enrichment fold change relative to the control.

genes (Fig. 6D). Taken together, these results demonstrated that the RpoX protein could modulate the expression of flagellum-, biofilm-, and hemolysis-related genes in *V. alginolyticus*.

Zebrafish were used as a model system to test the impact of RpoE and RpoX on the virulence of *V. alginolyticus*. The 50% lethal dose (LD_{50}) values for the WT and Δ*rpoE* strains were 2.5×10^5 and 6.6×10^6 CFU/fish at 30°C, respectively, demonstrating an essential role of *rpoE* in *V. alginolyticus* virulence. However, the Δ*rpoX* strain exhibited an LD_{50} value of 1.8×10^5 CFU/fish (Fig. 6E), indicating that the deletion of *rpoX* did not significantly impair virulence toward fish. Collectively, these data illuminated the RpoE-RpoX-centered regulatory cascades and their distinct and overlapping regulatory functions in pathogenesis and in stress responses in *V. alginolyticus*.

DISCUSSION

Sigma factors can interact with the RNA polymerase (RNAP) core enzyme to generate an RNAP holoenzyme and initiate the transcription of a specific set of genes responsible for the stress response and virulence (26). Here, we identified the *rpoX* gene, included as part of the regulon of RpoE, and genetic analysis showed that RpoX lacked the region 3 domain that is present in the RpoS protein. We speculate that the RpoX protein might be a paralog of RpoH because they share the same functional domains (see Fig. S1A in the supplemental material) and 45% overall similarity, and both proteins are alternative sigma factors under subhierarchical control by RpoE and are involved in high-temperature and low-osmotic-stress responses (Fig. 1 and 2) (3). Moreover, the high expression level of RpoH seems to be able to rescue the growth defects of the Δ*rpoX* strain under high-temperature and low-osmotic-stress conditions (Fig. 1F). Further experiments with the *rpoH* null mutant to compare the regulons of RpoH and RpoX as well as their recognized promoters will validate their homology and functional redundancy in response to stresses.

The dozens of established alternative sigma factors, i.e., *rpoH*, *rpoN*, *rpoE*, and *rpoS*, etc., are all subject to tight regulation under various specific physiological conditions (12). Interestingly, our data indicated that the expression of *rpoX* was induced under both low-osmotic-stress conditions and high temperatures (Fig. 1). Although how these

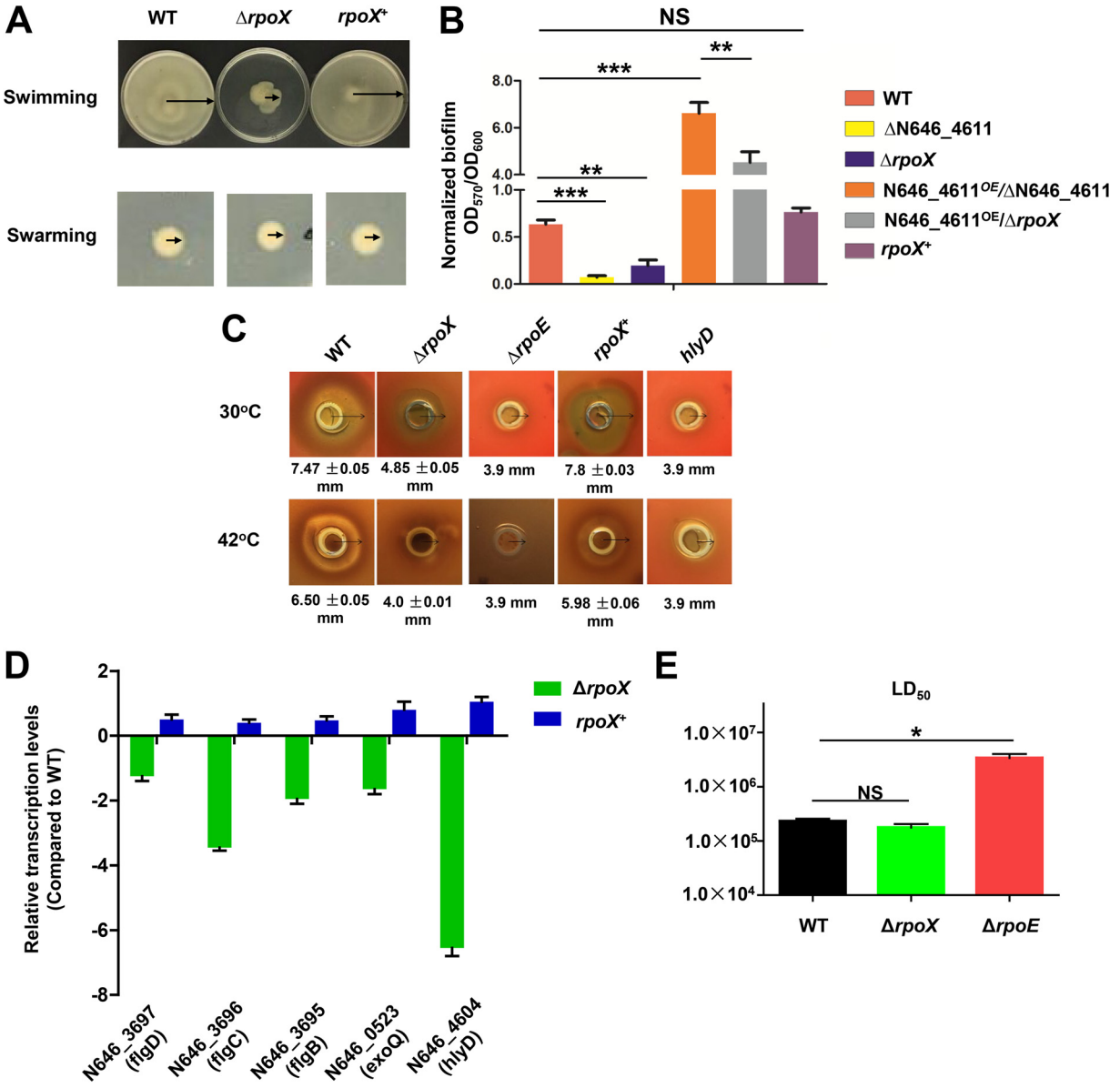

FIG 6 RpoX positively regulates motility, biofilm formation, and hemolytic activities. (A) Motility assays of WT, Δ*rpoX*, and *rpoX*$^+$ strains. Diluted cultures were spotted onto swimming and swarming plates (containing 0.3% and 1.5% agar, respectively) and incubated for 48 h or 12 h at 42°C. Three independent cultures were used for each strain, and a representative result is displayed. (B) Assays of biofilm formation by different strains. For WT, ΔN646_4611, Δ*rpoX*, and *rpoX*$^+$ strains, biofilm formation in glass tubes containing LBS medium after 48 h of culturing was assayed. N646_4611^{OE}/ΔN646_4611 and N646_4611^{OE}/Δ*rpoX* strains were cultured in LBS medium with 0.04% L-arabinose for 48 h. The results are presented as the means ± SD ($n = 3$). **, $P < 0.01$; ***, $P < 0.001$; NS, not significant (by *t* test). (C) Hemolytic activities of WT, Δ*rpoX*, Δ*rpoE*, *rpoX*$^+$, and Δ*luxR* strains grown on sheep blood agar plates at 30°C (top) and at 42°C (bottom). (D) qRT-PCR analysis of the transcripts of the selected genes. Total RNA was isolated from the Δ*rpoX* and *rpoX*$^+$ strains after 12 h of growth in liquid culture. The results are presented as the means ± SD ($n = 3$). (E) Median lethal dose (LD_{50}) of WT, Δ*rpoX*, and Δ*rpoE* strains in zebrafish. Series of dilutions of WT, Δ*rpoX*, and Δ*rpoE* strains were intramuscularly inoculated into fish that were acclimated at 30°C for 4 weeks. A total of 30 fish were used for each of the dilutions. The infected fish were cultivated at 30°C and monitored for 7 days. The results are presented as the means ± SD ($n = 3$). *, $P < 0.05$ (by *t* test).

conditions exert influences on *rpoX* expression warrants further investigation, these observations suggested that this alternative sigma factor may be induced *in vivo* in marine animals or at extremely high sea surface temperatures, orchestrate gene expression in response to these stresses, and thus facilitate *Vibrio* adaptation under both *in vivo* and *in vitro* conditions of the hosts. Indeed, our further transcriptomic and phenotypic investigations indicated that RpoX was involved in the expression of various genes (Table 1 and Fig. 6). We thus unraveled a novel RpoX-involved

signal transduction pathway in vibrios to respond to low-osmotic-stress and high-temperature stimuli.

As an alternative sigma factor, RpoE is released via regulated intramembrane proteolysis of the anti-sigma factor RseA triggered by membrane stresses (13) and has been found to be essential for stress adaptation and virulence in response to environmental stimuli in various bacterial pathogens, such as *V. parahaemolyticus*, *V. harveyi*, *V. cholerae*, and *Salmonella* (15, 16, 27–29). The RpoE protein can directly regulate the expression of the RpoH protein and is responsible for the high-temperature stress response of *V. alginolyticus* (3). In this study, we found that the RpoE protein can also bind directly to the promoter and control the expression of the RpoX protein (Fig. 2). RNA-seq was used to identify the regulons of the RpoX and RpoE proteins at a high temperature (42°C). The results showed that the regulon of RpoE contains more genes than that of RpoX (Fig. 3A and B), which, in addition to the result that the RpoE protein can directly bind to the promoter of *rpoX* and trigger the expression of *rpoX* (Fig. 2B to D), further confirmed that RpoX is at the subhierarchical level in the RpoE regulatory cascade; i.e., RpoE may act upstream of the regulatory cascade of RpoX. ChIP-seq and EMSA results also showed that the *rpoX* gene can be directly regulated by RpoX (Fig. 2C).

Sigma factors have been reported to be essential regulators of virulence, and we found that many virulence-associated genes, i.e., the genes encoding hemolysin (N646_4604 and N646_3664), exopolysaccharides (N646_0523 and N646_0530), flagella (N646_1186, N646_2929, N646_1338, N646_1844, N646_2932, and N646_2936), and type I pili (N646_3227, N646_3225, N646_3224, and N646_3223) (Fig. 7), were regulated by RpoX or RpoE at high temperatures (Table 1). Accordingly, our study has shown that RpoX was involved in the pathogenesis-related regulation of motility, biofilm formation, and hemolytic activity (Fig. 6). Although the Δ*rpoX* mutant strain did not show apparent attenuation of lethality to zebrafish (Fig. 6E), it may be related to the pathogenesis process and virulence factor production in an undiscerned manner in response to stresses such as reactive oxygen species (ROS), osmotic changes, and temperatures (23). In *V. alginolyticus*, swimming ability was increased in the Δ*rpoE* strain at high temperatures (3), while this ability was significantly decreased in the Δ*rpoX* strain, suggesting that the regulation of motility by RpoX is independent of RpoE. Taken together, these analyses indicate that RpoX might modulate stress adaptation in an RpoE-dependent manner but regulate motility in an RpoE-independent manner. RNA-seq analyses also support the idea that RpoX might be involved in some RpoE-independent processes and signaling in *V. alginolyticus* (Table 1).

We thus present a putative scenario where RpoE and RpoX are involved in the heat stress response in *V. alginolyticus* (Fig. 7). The release of RpoE protein tethered to the inner membrane into the cytoplasm could be a response to high temperatures, triggering the degradation of the anti-sigma factor RseA (3, 16, 27, 28). The RpoE protein can directly bind to the promoter of *rpoX* and control the expression of this gene. The RpoE sigma factor can directly regulate *rpoH* and *rpoX* to mediate the high-temperature response. However, our RNA-seq analysis indicated that, in addition to the high-temperature response, the RpoX protein may be able to regulate many other pathways, such as those associated with virulence processes, ABC transport, flagellar assembly, F-type ATPases, carbon metabolism, type I/II secretion systems, and two-component systems (Fig. 7 and Table 1). In addition, RpoX regulates its own expression, a feature exhibited by many other alternative sigma factors (21, 30). The question remains regarding how RpoE responds to heat or other stresses to orchestrate the expression of *rpoX*, *rpoH*, and the gene encoding itself, *rpoE*, as well as other alternative sigma factors.

In summary, this investigation presented an RpoE-RpoX-centered heat stress response regulatory cascade. These data facilitate an improved understanding of the regulatory networks of various alternative sigma factors contributing to their distinct and overlapping regulatory functions in stress responses and virulence in the pathogen *V. alginolyticus*.

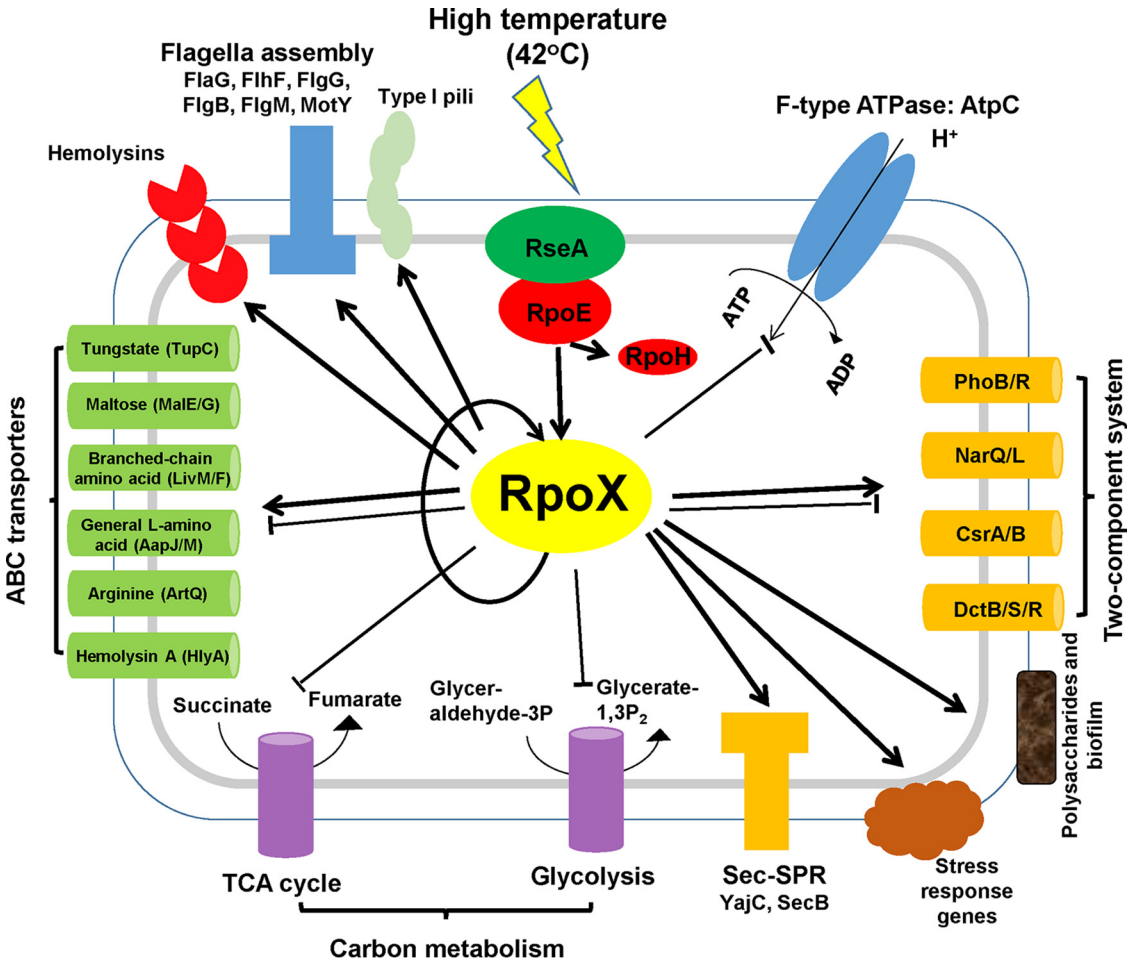

FIG 7 Schematic of the regulation network of RpoX in *V. alginolyticus*. Pathway analysis was performed with the Kobas 3.0 algorithm. The various pathways and their respective cellular locations, as well as the regulatory roles of RpoX, are illustrated with arrows (activation) or bar-ended lines (repression) and are discussed in the text. 3P, 3-phosphate; TCA, tricarboxylic acid.

MATERIALS AND METHODS

Bacterial strains, plasmids, and culture conditions. The strains and plasmids used in this study are listed in Table 2. The *V. alginolyticus* strains were grown in Luria-Bertani (LB) broth containing 3% sodium chloride (LBS broth) at 30°C as the normal growth conditions. *Escherichia coli* DH5α (λ*pir*), *E. coli* SM10 (λ*pir*), and *E. coli* BL21(DE3) were grown in LB broth at 37°C. When appropriate, the medium was supplemented with carbenicillin (100 μg ml^{-1}), chloramphenicol (25 μg ml^{-1}), kanamycin (50 μg ml^{-1}), or L-arabinose (0.2 mg ml^{-1}).

Deletion mutant and complemented strain construction. In-frame deletion mutants were generated as described in a previous study (10). The fragment was cloned into the XbaI sites of the suicide vector pDM4 (31), and the resulting plasmid was transformed into *E. coli* DH5α λ*pir*. After sequencing, pDM4 derivatives were transformed into *E. coli* SM10 λ*pir*. This plasmid was introduced into *V. alginolyticus* by conjugation. The double-crossover recombinant was selected on LBS agar containing 15% sucrose. The mutation was confirmed by PCR and sequencing. A fragment containing the intact *rpoX* gene (a 282-bp fragment of the promoter adjoining the start codon "ATG" and the open reading frame [ORF]) and the Flag sequence was cloned into the plasmid pBAD33 to construct a complementation strain (3).

Immunoblot analysis. For the immunoblot assay, supernatants and bacterial cell pellets were harvested at the same optical density measured at 600 nm (OD_{600}). Next, 15 μl of each sample was loaded onto a 12% denaturing polyacrylamide gel, and proteins were resolved by electrophoresis and transferred to a polyvinylidene difluoride (PVDF) membrane (Millipore, Bedford, MA). The membranes were blocked with a 10% skim milk powder solution, incubated with a 1:2,000 dilution of Flag-specific (Sigma-Aldrich, St. Louis, MO) mouse antiserum, and incubated with a 1:2,000 dilution of horseradish peroxidase-conjugated goat anti-mouse IgG (Santa Cruz Biotechnology, CA). Finally, the blots were visualized with an enhanced chemiluminescence reagent (Thermo Fisher Scientific Inc., Waltham, MA).

Growth curves. Bacteria were incubated overnight and then diluted 1:100 in 50 ml of fresh LBS medium. The bacteria were then grown in LBS medium at 30°C or 42°C or in LB broth containing 0.5%

TABLE 2 Bacterial strains and plasmids used in this study

Strain or plasmid	Description[a]	Source or reference
Strains		
Escherichia coli		
DH5α λ*pir*	Host for π-requiring plasmids	Laboratory collection
SM10 λ*pir*	Host for π-requiring plasmids; conjugal donor; Km^r	40
BL21(DE3)	Host strain for protein expression	Novagen
BL21/pET22b::*rpoE*	BL21; expression of RpoE; Km^r	This study
BL21/pET22b::*rpoX*	BL21; expression of RpoX; Km^r	This study
Vibrio alginolyticus		
EPGS	Wild type; fish isolate; CCTCC strain AB 209306; Carb^r	Laboratory collection
Δ*rpoE*	EPGS; in-frame deletion in *rpoE*; Carb^r	3
Δ*rpoX*	EPGS; in-frame deletion in *rpoX*; Carb^r	This study
Δ*luxR*	EPGS; in-frame deletion in *luxR*; Carb^r	3
Δ*hlyD*	EPGS; *hlyD* disrupted; Carb^r Cm^r	This study
ΔN646_4611	EPGS; GGDEF domain deletion in EPGS_03411; Carb^r	This study
Δ*asp*	EPGS; disrupted in *asp*; Carb^r Cm^r	6
rpoX$^+$	Δ*rpoX*; pBAD33 carrying the intact *rpoX* gene	This study
N646_4611^{OE}/ΔN646_4611	ΔN646_4611; pBAD33 carrying the ORF of N646_4611	This study
N646_4611^{OE}/Δ*rpoX*	Δ*rpoX*; pBAD33 carrying the ORF of EPGS_03411; Carb^r Cm^r	This study
WT/pBAD33::Flag	EPGS; pBAD33 carrying the Flag gene; Carb^r Cm^r	This study
WT/pBAD33::P$_{rpoX}$-Flag	EPGS; pBAD33 carrying the intact *rpoX*-Flag gene; Carb^r Cm^r	This study
Δ*rpoE*/pBAD33::P$_{rpoX}$-Flag	Δ*rpoE*; pBAD33 carrying the intact *rpoX*-Flag gene; Carb^r Cm^r	This study
Δ*rpoX*/pBAD33::P$_{rpoX}$-Flag	Δ*rpoX*; pBAD33 carrying the intact *rpoX*-Flag gene; Carb^r Cm^r	This study
WT/pDM8::P$_{rpoX}$	EPGS; pDM8 carrying the promoter region of *rpoX*; Carb^r Cm^r	This study
Δ*luxO*/pDM8::P$_{rpoX}$	Δ*luxO*; pDM8 carrying the promoter region of *rpoX*; Carb^r Cm^r	This study
Δ*luxR*/pDM8::P$_{rpoX}$	Δ*luxR*; pDM8 carrying the promoter region of *rpoX*; Carb^r Cm^r	This study
Plasmids		
pDM4	Suicide vector; *pir* dependent; R6K; SacBR; Cm^r	41
pDM8	pSup202 derivative containing promoterless *lacZ*; Cm^r Tc^r	42
pBAD33	Carrying a *mob* gene in pBAD33; Cm^r	3
pET28a	Expression vector; Km^r	Novagen
pDM4::*rpoX*	pDM4 with *rpoX* fragment deleted from nt 4–576; Cm^r	This study
pDM4::N646_4611	pDM4 with GGDEF fragment deleted from nt 27–234; Cm^r	This study
pBAD33::P$_{rpoX}$-Flag	Plasmid expressing *rpoX*-Flag driven by P$_{rpoX}$; Cm^r	This study
pBAD33::Flag	pBAD33 derivative Flag expression plasmid; Cm^r	This study
pBAD33::N646_4611	pBAD33 derivative EPGS_03411 expression plasmid; Cm^r	This study
pDM8::P$_{rpoX}$	pDM8 carrying the promoter region of *rpoX*; Cm^r	This study
pET22b::*rpoE*	pET22b carrying the *rpoE* ORF; Km^r	This study
pET22b::*rpoX*	pET22b carrying the *rpoX* ORF; Km^r	This study

[a]nt, nucleotides.

NaCl at 30°C, and live bacterial counts were determined at 2, 4, 6, 8, 10, 12, and 24 h. At each time point, 100 μl of fresh culture was serially diluted with phosphate-buffered saline (PBS), and the dilutions were spread onto plates containing solidified LBS medium. The live bacterial count for each plate was obtained after cultivation for 12 h at 30°C.

Total RNA extraction. Bacteria were incubated overnight and then diluted 1:100 in LBS medium. The bacteria were then grown at 30°C or 42°C and harvested after 9 h. Total RNA was isolated using an RNA extraction kit (Tiangen, Beijing, China). The RNA samples were digested with DNase I (Promega, Madison, WI, USA) to eliminate genomic DNA contamination. Before reverse transcription, regular PCR was routinely performed using the isolated RNA sample as a template to confirm that there was no DNA contamination.

5′ RACE. We performed 5′ RACE (rapid amplification of cDNA ends) experiments as previously described (3). Six micrograms of total RNA was subjected to dephosphorylation using tobacco acid pyrophosphatase (TAP) (Epicentre) for 60 min at 37°C. The RNA oligonucleotide linker was ligated to total RNA using T4 RNA ligase (New England Biolabs, Beverly, MA, USA) according to the manufacturer's instructions. cDNA was synthesized using avian myeloblastosis virus (AMV) reverse transcriptase (RT) (TaKaRa) according to the manufacturer's instructions, using a random primer. First-round PCR amplification was performed using RACE-adapter and the primer *rpoX*-RACE (Table 3), and second-round PCR amplification was performed using RACE-adapter-nested primers and *rpoX*-RACE-nested primers (Table 3). The single resulting band was extracted, subcloned, and sequenced.

Quantitative real-time reverse transcription-PCR. Equal amounts of RNA (1 μg) were used to generate cDNA (Toyobo, Tsuruga, Japan) using 6-mer random primers. Three independent qRT-PCR experiments were performed, and each experiment was run in triplicate. The primers for qRT-PCR (Table 3) were designed using the NCBI primer selection tool with predicted product sizes ranging from 100 to 200 bp. The reactions were run on an Applied Biosystems 7500 real-time system (Applied Biosystems), and the transcript levels were normalized to the 16S rRNA levels in each sample by using the $\Delta\Delta C_T$ method.

TABLE 3 Primers used in this study

Primer	Sequence (5′–3′)
Δ*rpoX*-up-F	CTAGTGGGGCCCTTCTAGATGCAATTCATTTGAGTATCAGTTTGG
Δ*rpoX*-up-R	GCTAAAAATCTGACAGTTCATCCGTGACAGCTCGG
Δ*rpoX*-down-F	TGAACTGTCAGATTTTTAGCCCCTTATCCTAGCCG
Δ*rpoX*-down-R	CGGGAGAGCTCAGGTTACCCCTGACTTTAACCTTCAACACATCGA
Δ*rpoX*-out-F	TGCTGGAGACCGAGCAATAGTTGCC
Δ*rpoX*-out-R	ACGAGCCATTTAATGGTGCAGAGCA
Δ*rpoX*-in-F	ATGAAAGAATCGTTGTCAGTTGGGA
Δ*rpoX*-in-R	TTAAACCCAACCATCGAATCGGAGA
ΔN646_4611-up-F	GAGCTCAGGTTACCCGCATGCAAGATCTATTATGGACTTTGGCGCAGTCATAATG
ΔN646_4611-up-R	ATAACTTGGAACGTCATCTCCAGCAATTGCTGATTG
ΔN646_4611-down-F	TGGAGATGACGTTCCAAGTTATAACAGACTGTCAGC
ΔN646_4611-down-R	CCCTCGAGTACGCGTCACTAGTGGGGCCCTGACAGCTCGGAACCTAGCAAAGCAT
ΔN646_4611-out-F	GAGTACGCGGCGAACAACCAAATCG
ΔN646_4611-out-R	CGAGACAACAAATCAATGCCCAC
ΔN646_4611-in-F	CACCTGATTGAGCAATTGGC
ΔN646_4611-in-R	GTAAACTCAGGATAGTAAGC
rpoX-Flag-F	CCATACCCGTTTTTTTGGGCTAGCGAATTCAGGCCAATTTGCGTACAAATACTAT
rpoX-Flag-R1	CTTGTCGTCGTCGTCCTTGTAGTCAACCCAACCATCGAATCGGAGACGT
Flag-R2	GGTCAGCATGGGTACCTTTCTCCTCTTTAATTACTTGTCGTCGTCGTCCTTGTAGTC
N646_4611-Flag-F	CCATACCCGTTTTTTTGGGCTAGCGAATTCTTCAGCCGTAAAATGAAGCATAGAG
N646_4611-Flag-R	CTTGTCGTCGTCGTCCTTGTAGTCATTCACTTGACGAAGCGCAGGTTGA
rpoE-pET22b-F	ATCGGATCCGATGAACGAGCAGCTGACCGATC
rpoE-pET22b-R	ATATGTCGACGCGTTGCAAAAGAGGTCTGATT
rpoX-pET22b-F	ATCGGATCCATGAAAGAATCGTTGTCAGTTGGGA
rpoX-pET22b-R	ATATGTCGACAACCCAACCATCGAATCGGAGA
pDM8-P*rpoX*-F	ATCCCGGGAGGCCAATTTGCGTACAAATACTTG
pDM8-P*rpoX*-R	ATCCCGGGTGACAGTTCATCCGTGACAGCTCGG
rpoX-RACE-nested	TCACGAGACAACAAATCAATGCCCA
rpoX-RACE	CAACATTTCGCGCGCTTCTTCATCA
RACE-adapter	GCGCGAATTCCTGTAGA
RACE-adapter2	GCGCGAATTCCTGTAGAACGAAC
RNA-Linker	AUAUGCGCGAAUUCCUGUAGAACGAACACUAGAAGAAA
P_{rpoX}cy5-F	TGCCTGCAGGTCGACGATCGGCCAATTTGCGTACAAATACTTG
P_{rpoX}cy5-R	TGACAGTTCATCCGTGACAGCTCGG
P_{N646_4603}cy5-F	TGCCTGCAGGTCGACGATCTCGACTGCTGTTTTTCTTCT
P_{N646_4603}cy5-R	ATTTATCATTATCCCACCGCAC
P_{N646_4601}cy5-F	TGCCTGCAGGTCGACGATCAATCGACAACAAAGTATACAAACCAAGAC
P_{N646_4601}cy5-R	CTCTAGTTCTGACTCCGGCACAT
P_{N646_1623}cy5-F	TGCCTGCAGGTCGACGATCAGACTCTTTTGCAAATGGCTTG
P_{N646_1623}cy5-R	TTTTTAAATTCCTAGAATAAACTGATACTAAATAAAT
gyrB cy5-F	TGCCTGCAGGTCGACGATCGCACTATCAGAGAAAGTTGAGC
gyrB cy5-R	CCACCTTCATACATGAAGTGATCA
rpoE-qRT-F	TGTTGCTCAAGGGCGTAGAC
rpoE-qRT-R	CGATTGCACTGAACACCACC
rpoX-qRT-F	TAATGAACAATGGCCGCACG
rpoX-qRT-R	GCTCTGCTTTCACCCCTGAG
rpoH-qRT-F	GCGAGTTAGGTGTTGAGCCT
rpoH-qRT-R	ATAGCATCGGCGCTGTGTAA
N646_3697qRTF	GCTCAGTTCTCGCAGGTACA
N646_3697qRTR	AACAAGGCCCGCTGTTGATA
N646_3696qRTF	AGAGAAGCGTTTTGAGCCGA
N646_3696qRTR	ATTCGTTTCGAAGCTGCGTG
N646_3695qRTF	GTCCTCGCCAGTAACCTAGC
N646_3695qRTR	CACCGGTTTGTTCACACCAC
N646_0523qRTF	CGCGTCCCTTCAACCAAATC
N646_0523qRTR	ACAGCTCGCACAGATGTCAA
N646_4604qRTF	GCAGTACCGAGACTTGGTGG
N646_4604qRTR	GTAAACCACGAGGCGATCCA
16S RNA-qRT-F	AAAGCACTTTCAGTCGTGAGGAA
16S RNA-qRT-R	TGCGCTTTACGCCCAGTAAT

Electrophoretic mobility shift assay. The purification of 6×His-tagged RpoE and RpoX from *E. coli* BL21(DE3) with nickel affinity chromatography was performed as previously described (3). For electrophoretic mobility shift assays (EMSAs), purified 6×His-tagged RpoE or RpoX was incubated with different Cy5-labeled DNA probes (Table 2) in 20 μl of loading buffer (10 mM NaCl, 0.1 mM dithiothreitol [DTT], 0.1 mM EDTA, 10 mM Tris [pH 7.4]). After the mixture was incubated at 25°C for 30 min, the samples were

resolved using 6% polyacrylamide gel electrophoresis in 0.5× TBE (Tris-boric acid-EDTA) buffer on ice at 100 V for 120 min. Next, the gels were scanned using a Typhoon FLA 9500 instrument (GE Healthcare, Uppsala, Sweden).

RNA-seq analysis. For RNA-seq analysis of the Δ*rpoX* or Δ*rpoE* strain, bacteria were incubated overnight and then diluted 1:100 in LBS medium. The bacteria were then grown at 42°C and harvested after 9 h. The subsequent procedures and statistical analysis were performed as previously described (32).

ChIP-seq analysis. For the ChIP-seq analysis of RpoX, the pBAD33::P_{rpoX}-Flag and pBAD33::Flag plasmids, encoding RpoX-Flag and the Flag tag alone (control), respectively, were transferred to the Δ*rpoX* strain. Cultures of each strain grown overnight in LBS medium at 42°C or in LB medium containing 0.5% NaCl at 30°C were diluted (1:100) in 50 ml of fresh LBS medium with 0.04% L-arabinose. After 9 h of growth with shaking, the protein-DNA complexes in the bacterial cells were fixed *in vivo* with rifampin at a final concentration of 150 μg/ml under the corresponding conditions for 20 min (33) and then cross-linked *in vivo* with 1% formaldehyde at room temperature for 10 min. Cross-linking was stopped by the addition of 125 mM glycine. The following procedures and statistical analysis were performed as previously described (34). Briefly, bacterial cells were sonicated in SDS lysis buffer, and the DNA was fragmented to 100 to 500 bp and immunoprecipitated (IP) with Flag-labeled beads. IP DNA was collected in elution buffer, followed by reversion of the DNA-protein cross-links and purification of the DNA by phenol-chloroform. DNA fragments were used for library construction with the VAHTS Turbo DNA library prep kit and then sequenced with a MiSeq sequencer (Illumina, San Diego, CA). ChIP-seq reads were mapped to the *V. alginolyticus* EPGS genome. The enriched peaks were identified using MACS software (35), followed by MEME analysis to generate the RpoX-binding motif (36). KEGG pathway analysis was performed with Kobas 3.0 to illustrate the enriched gene function (37).

Motility, biofilm, and hemolytic activity assays. The motility assay was performed as previously described (10). Cultures grown overnight were diluted to an OD_{600} of 1.0 and then spotted onto LBS medium containing 0.3% (swimming) and 1.5% (swarming) agar. After incubation at 30°C for 12 h and 24 h, respectively, bacterial motility was observed. The experiments were performed at least three times, and one representative result is shown.

The biofilm assay was performed as previously described (10). Cultures grown overnight (50 μl) were diluted to 5 ml in LBS medium in glass tubes and incubated at 30°C without shaking for 48 h. A total of 0.04% L-arabinose, which exerts no apparent influence on biofilm formation of the WT, was added to LBS medium to induce the pBAD promoter. The total biofilm was measured by 2% crystal violet staining. The experiments were performed at least three times, and one representative result is shown.

Hemolytic activity assays were performed as previously described (4, 28, 38). *V. alginolyticus* strains were grown to mid-log phase in LBS medium at 30°C. The bacterial cells were centrifuged at 500 × *g*, washed three times with PBS, and then resuspended with PBS to a final concentration of 0.5×10^9 CFU/ml. For the blood agar assay, a suspension of 5% defibrinated sheep blood erythrocytes was added to LBS agar medium (45°C to 50°C), mixed gently, and poured into plates. Pellets of 5-μl bacterial suspensions were dropped onto the blood agar plates. The plates were incubated at 30°C or 42°C for 12 h. The experiments were performed at least three times, and one representative result is shown.

LD_{50} determination. Median lethal dose (LD_{50}) determination for the WT, Δ*rpoX*, or Δ*rpoE* strain in the zebrafish infection model was performed as previously described (39). Healthy fish, each weighing approximately 0.25 g, were obtained from a commercial farm and acclimatized to the laboratory conditions for at least 15 days. Zebrafish were anesthetized with tricaine methanesulfonate (catalog no. MS-222; Sigma-Aldrich) at a concentration of 80 mg/liter. Groups of 10 fish each were injected intramuscularly with bacterial cells adjusted to the required concentrations. Fish mortality was monitored over a period of 7 days postinfection. Fish injected with PBS only served as negative controls. The LD_{50} values were calculated as described previously (39). The animal work presented here was approved by the Animal Care Committee, East China University of Science and Technology (approval no. 2006272).

Statistical analysis. GraphPad Prism (version 6) was used to perform the statistical analyses. To compare gene expression or CFU between the groups, a two-tailed Student's unpaired *t* test was used. A P value of <0.05 was considered significant.

Data availability. The sequence reads were deposited in the SRA database under accession no. SRP152034.

SUPPLEMENTAL MATERIAL

Supplemental material for this article may be found at https://doi.org/10.1128/AEM.00234-19.

SUPPLEMENTAL FILE 1, PDF file, 0.2 MB.

ACKNOWLEDGMENT

This work was supported by grants from the National Natural Science Foundation of China (no. 31772893 to Y.M. and 31772891 to Q.W.), the Ministry of Agriculture of China (CARS-47-G17), and the Science and Technology Commission of Shandong and Shanghai Municipality (2017CXGC0103 and 17391902000).

REFERENCES

1. Austin B. 2010. Vibrios as causal agents of zoonoses. Vet Microbiol 140:310–317. https://doi.org/10.1016/j.vetmic.2009.03.015.
2. Jacobs Slifka KM, Newton AE, Mahon BE. 2017. *Vibrio alginolyticus* infections in the USA, 1988–2012. Epidemiol Infect 145:1491–1499. https://doi.org/10.1017/S0950268817000140.
3. Gu D, Guo M, Yang MJ, Zhang YX, Zhou XH, Wang QY. 2016. A σ^E-mediated temperature gauge controls a switch from LuxR-mediated virulence gene expression to thermal stress adaptation in *Vibrio alginolyticus*. PLoS Pathog 12:e1005645. https://doi.org/10.1371/journal.ppat.1005645.
4. Wang QY, Liu Q, Ma Y, Rui HP, Zhang YX. 2007. LuxO controls extracellular protease, haemolytic activities and siderophore production in fish pathogen *Vibrio alginolyticus*. J Appl Microbiol 103:1525–1534. https://doi.org/10.1111/j.1365-2672.2007.03380.x.
5. Rui HP, Liu Q, Ma Y, Wang QY, Zhang YX. 2008. Roles of LuxR in regulating extracellular alkaline serine protease A, extracellular polysaccharide and mobility of *Vibrio alginolyticus*. FEMS Microbiol Lett 285:155–162. https://doi.org/10.1111/j.1574-6968.2008.01185.x.
6. Rui HP, Liu Q, Wang QY, Ma Y, Liu H, Shi CB, Zhang YX. 2009. Role of alkaline serine protease, Asp, in *Vibrio alginolyticus* virulence and regulation of its expression by LuxO-LuxR regulatory system. J Microbiol Biotechnol 19:431–438. https://doi.org/10.4014/jmb.0807.404.
7. Cao XD, Wang QY, Liu Q, Liu H, He HH, Zhang YX. 2010. *Vibrio alginolyticus* MviN is a *luxO*-regulated protein and affects cytotoxicity towards EPC cells. J Microbiol Biotechnol 20:271–280.
8. Cao XD, Wang QY, Liu Q, Rui HP, Liu H, Zhang YX. 2011. Identification of a *luxO*-regulated extracellular protein Pep and its roles in motility in *Vibrio alginolyticus*. Microb Pathog 50:123–131. https://doi.org/10.1016/j.micpath.2010.12.003.
9. Zhao Z, Zhang LP, Ren CH, Zhao JJ, Chen C, Jiang X, Luo P, Hu CQ. 2011. Autophagy is induced by the type III secretion system of *Vibrio alginolyticus* in several mammalian cell lines. Arch Microbiol 193:53–61. https://doi.org/10.1007/s00203-010-0646-9.
10. Sheng LL, Lv YZ, Liu Q, Wang QY, Zhang YX. 2013. Connecting type VI secretion, quorum sensing, and c-di-GMP production in fish pathogen *Vibrio alginolyticus* through phosphatase PppA. Vet Microbiol 162:652–662. https://doi.org/10.1016/j.vetmic.2012.09.009.
11. Bashyam MD, Hasnain SE. 2004. The extra cytoplasmic function sigma factor: role in bacterial pathogenesis. Infect Genet Evol 4:301–308. https://doi.org/10.1016/j.meegid.2004.04.003.
12. Kazmierczak MJ, Wiedmann M, Boor KJ. 2005. Alternative sigma factors and their roles in bacterial virulence. Microbiol Mol Biol Rev 69:527–543. https://doi.org/10.1128/MMBR.69.4.527-543.2005.
13. Sineva E, Savkina M, Ades SE. 2017. Themes and variation in gene regulation by extracytoplasmic function (ECF) sigma factors. Curr Opin Microbiol 36:128–137. https://doi.org/10.1016/j.mib.2017.05.004.
14. Mathur J, Davis BM, Waldor MK. 2007. Antimicrobial peptides activate the *Vibrio cholerae* sigma E regulon through an OmpU-dependent signaling pathway. Mol Microbiol 63:848–858. https://doi.org/10.1111/j.1365-2958.2006.05544.x.
15. Davis BM, Waldor MK. 2009. High-throughput sequencing reveals suppressors of *Vibrio cholerae rpoE* mutations: one fewer porin is enough. Nucleic Acids Res 37:5757–5767. https://doi.org/10.1093/nar/gkp568.
16. Haines-Menges B, Whitaker WB, Boyd EF. 2014. Alternative sigma factor RpoE is important for *Vibrio parahaemolyticus* cell envelope stress response and intestinal colonization. Infect Immun 82:3667–3677. https://doi.org/10.1128/IAI.01854-14.
17. Merrikh H, Ferrazzoli AE, Bougdour A, Olivier-Mason A, Lovett ST. 2009. A DNA damage response in *Escherichia coli* involving the alternative sigma factor, RpoS. Proc Natl Acad Sci U S A 106:611–616. https://doi.org/10.1073/pnas.0803665106.
18. Landini P, Egli T, Wolf J, Lacour S. 2014. Sigma S, a major player in the response to environment stresses in *Escherichia coli*: role, regulation and mechanisms of promoter recognition. Environ Microbiol Rep 6:1–13. https://doi.org/10.1111/1758-2229.12112.
19. Wurm P, Tutz S, Mutsam B, Vorkapic D, Heyne B, Grabner C, Kleewein K, Halscheidt A, Schild S, Reidl J. 2017. Stringent factor and proteolysis control of sigma factor RpoS expression in *Vibrio cholerae*. Int J Microbiol 307:154–165. https://doi.org/10.1016/j.ijmm.2017.01.006.
20. Tian Y, Wang QY, Liu Q, Ma Y, Cao XD, Zhang XY. 2008. Role of RpoS in stress survival, synthesis of extracellular autoinducer 2, and virulence in *Vibrio alginolyticus*. Arch Microbiol 190:585–594. https://doi.org/10.1007/s00203-008-0410-6.
21. Slamti L, Livny J, Waldor MK. 2007. Global gene expression and phenotypic analysis of a *Vibrio cholerae rpoH* deletion mutant. J Bacteriol 189:351–362. https://doi.org/10.1128/JB.01297-06.
22. Rhodius VA, Suh WC, Nonaka G, West J, Gross CA. 2006. Conserved and variable functions of the σ^E stress response in related genomes. PLoS Biol 4:e2. https://doi.org/10.1371/journal.pbio.0040002.
23. Zhao JJ, Chen C, Zhang LP, Hu CQ. 2009. Cloning, identification, and characterization of the *rpoS*-like sigma factor *rpoX* from *Vibrio alginolyticus*. J Biomed Biotechnol 2009:126986. https://doi.org/10.1155/2009/126986.
24. Caly DL, Bellini D, Walsh MA, Dow JM, Ryan RP. 2015. Targeting cyclic di-GMP signaling: a strategy to control biofilm formation? Curr Pharm Des 21:12–24. https://doi.org/10.2174/1381612820666140905124701.
25. Kim JS, Song S, Lee M, Lee S, Lee K, Ha NC. 2016. Crystal structure of a soluble fragment of the membrane fusion protein HlyD in a type I secretion system of Gram-negative bacteria. Structure 24:477–485. https://doi.org/10.1016/j.str.2015.12.012.
26. Mauri M, Klumpp S. 2014. A model for sigma factor competition in bacterial cells. PLoS Comput Biol 10:e1003845. https://doi.org/10.1371/journal.pcbi.1003845.
27. Kovacikova G, Skorupski K. 2002. The alternative sigma factor σ^E plays an important role in intestinal survival and virulence in *Vibrio cholerae*. Infect Immun 70:5355–5362. https://doi.org/10.1128/IAI.70.10.5355-5362.2002.
28. Rattanama P, Thompson JR, Kongkerd N, Srinitiwarawong K, Vuddhakul V, Mekalanos JJ. 2012. Sigma E regulators control hemolytic activity and virulence in a shrimp pathogenic *Vibrio harveyi*. PLoS One 7:e32523. https://doi.org/10.1371/journal.pone.0032523.
29. Li J, Nakayasu ES, Overall CC, Johnson RC, Kidwai AS, McDermott JE, Ansong C, Heffron F, Cambronne ED, Adkins JN. 2015. Global analysis of Salmonella alternative sigma factor E on protein translation. J Proteome Res 14:1716–1726. https://doi.org/10.1021/pr5010423.
30. Rhodius VA, Mutalik VK. 2010. Predicting strength and function for promoters of the *Escherichia coli* alternative sigma factor, σ^E. Proc Natl Acad Sci U S A 107:2854–2859. https://doi.org/10.1073/pnas.0915066107.
31. Gibson DG, Young L, Chuang RY, Venter JC, Hutchison CA, Smith HO. 2009. Enzymatic assembly of DNA molecules up to several hundred kilobases. Nat Methods 6:343–345. https://doi.org/10.1038/nmeth.1318.
32. Liu Y, Zhao LY, Yang MJ, Yin KY, Zhou XH, Leung KY, Liu Q, Zhang YX, Wang QY. 2017. Transcriptomic dissection of the horizontally acquired response regulator EsrB reveals its global regulatory roles in the physiological adaptation and activation of T3SS and the cognate effector repertoire in *Edwardsiella piscicida* during infection toward turbot. Virulence 8:1355–1377. https://doi.org/10.1080/21505594.2017.1323157.
33. Herring CD, Raffaelle M, Allen TE, Kanin EI, Landick R, Ansari AZ, Palsson BØ. 2005. Immobilization of *Escherichia coli* RNA polymerase and location of binding sites by use of chromatin immunoprecipitation and microarrays. J Bacteriol 187:6166–6174. https://doi.org/10.1128/JB.187.17.6166-6174.2005.
34. Gu D, Liu H, Yang Z, Zhang Y, Wang Q. 2016. Chromatin immunoprecipitation sequencing technology reveals global regulatory roles of low-cell-density quorum-sensing regulator AphA in the pathogen *Vibrio alginolyticus*. J Bacteriol 198:2985–2999. https://doi.org/10.1128/JB.00520-16.
35. Feng JX, Liu T, Qin B, Zhang Y, Liu XL. 2012. Identifying ChIP-seq enrichment using MACS. Nat Protoc 7:1728–1740. https://doi.org/10.1038/nprot.2012.101.
36. Machanick P, Bailey TL. 2011. MEME-ChIP: motif analysis of large DNA datasets. Bioinformatics 27:1696–1697. https://doi.org/10.1093/bioinformatics/btr189.
37. Xie C, Mao XZ, Huang JJ, Ding Y, Wu JM, Dong S, Kong L, Gao G, Li CY, Wei LP. 2011. KOBAS 2.0: a Web server for annotation and identification of enriched pathways and diseases. Nucleic Acids Res 39:W316–W322. https://doi.org/10.1093/nar/gkr483.
38. Dasgupta N, Ashare A, Hunninghake GW, Yahr TL. 2006. Transcriptional induction of the *Pseudomonas aeruginosa* type III secretion system by low Ca^{2+} and host cell contact proceeds through two distinct signaling pathways. Infect Immun 74:3334–3341. https://doi.org/10.1128/IAI.00090-06.
39. Lv Y, Xiao J, Liu Q, Wu H, Zhang Y, Wang Q. 2012. Systematic mutation

analysis of two-component signal transduction systems reveals EsrA-EsrB and PhoP-PhoQ as the major virulence regulators in *Edwardsiella tarda*. Vet Microbiol 157:190–199. https://doi.org/10.1016/j.vetmic.2011.12.018.
40. Liang WL, Wang SX, Yu FG, Zhang LJ, Qi GM, Liu YQ, Gao SY, Kan B. 2003. Construction and evaluation of a safe, live, oral *Vibrio cholerae* vaccine candidate, IEM108. Infect Immun 71:5498–5504. https://doi.org/10.1128/IAI.71.10.5498-5504.2003.
41. Wang SY, Lauritz J, Jass J, Milton DL. 2002. A ToxR homolog from *Vibrio anguillarum* serotype O1 regulates its own production, bile resistance, and biofilm formation. J Bacteriol 184:1630–1639. https://doi.org/10.1128/JB.184.6.1630-1639.2002.
42. Croxatto A, Chalker VJ, Lauritz J, Jass J, Hardman A, Williams P, Camara M, Milton DL. 2002. VanT, a homologue of *Vibrio harveyi* LuxR, regulates serine, metalloprotease, pigment, and biofilm production in *Vibrio anguillarum*. J Bacteriol 184:1617–1629. https://doi.org/10.1128/JB.184.6.1617-1629.2002.